Confocal mapping of cortical inputs onto identified pyramidal neurons

Noritaka Ichinohe[1,2], James Hyde[1], Atsuko Matsushita[1], Kazumi Ohta[1], Kathleen S. Rockland[1,3]

[1]Lab for Cortical Organization and Systematics, RIKEN Brain Science Institute, 2-1 Hirosawa, Wako-shi, Saitama, 351-0198, Japan, [2]Department of Morphological Brain Science, Graduate School of Medicine, Kyoto University, Konoe-cho, Yoshida, Sakyo-ku, Kyoto 606-8501 Japan, [3]Graduate School of Science and Engineering, Saitama University, 255 Shimo-Okubo, Sakura-ku, Saitama City, Saitama 338-8570, Japan

TABLE OF CONTENTS

1. ABSTRACT

Using a confocal microscopy protocol, we carried out a microcircuitry investigation of cortical connections in monkey temporal cortex. Inputs were labeled by BDA injections in posterior area TE, and potential postsynaptic pyramidal neuron targets were labeled with EGFP, by injection of retrogradely transported adenovirus. We scored the number and distribution of putative contacts onto dendritic compartments of neurons in different layers. Initial results show that about 50% of apical dendrites of layer (L.) 6 neurons receive contacts, as they ascend through L.4 (n=1 brain), but only 30-35% of those from L.5 neurons (n=2). Basal dendrites of L.3 neurons also receive few contacts in L.4. This supports the role of layer 4 as an interlaminar relay in association cortex. In addition, our results indicate spatial heterogeneity in the occurrence and number of contacts, possibly due to subtype specificity in target preference. The maximum number of contacts, for a L.2 neuron projecting from anterior to posterior TE, was 29. This approach seems a useful alternative or complement to electron microscopic analyses of long distance connectivity.

2. INTRODUCTION: MICROCIRCUITRY OF LONG-DISTANCE CORTICAL CONNECTIONS

An important component of cortical organization and function is the long-distance connectivity. Thanks to decades of *in vivo* tracer injections, this is reasonably well understood at the basic level of what areas and structures are connected to others. Considerably less, however, is known at the level of individual neurons – questions such as rules of target specificity, how inputs are distributed along the dendritic domain, and how different inputs converge and interact. Even the terminology seems inadequate, more evocative than explicative; for example, the word "connections" tends to imply that some one thing is conveyed or transferred to some other one thing, like an electric cord and a wallplug. This is clearly not the case.

Long-distance connections can be roughly defined as extrinsic connections (from outside a given area), from cortical or subcortical sources. Deciphering this circuitry has met with several logistical handicaps, mainly having to do with problems of identification. In particular,

it has been difficult to label concurrently identified pre-synaptic inputs; identified postsynaptic targets, especially pyramidal cells; and individual contacts at a synaptic level. Only a few studies, mainly in rodent have approached simultaneous, high resolution labeling by using Golgi stains or intracellular labeling for neurons, anterograde tracer for inputs, and electron microscopy, sometimes *in vitro* after *in vivo* pre-labeling. Most of the available data for long-distance excitatory connections are limited to whether synapses contact dendritic shafts or spines, with little further information about exact dendritic location or exact identity of the targeted neuron (1-8). In this respect, the field lags significantly behind *in vitro* studies, where significant progress has been made concerning intrinsic local connectivity (9). (Even for the *in vitro* world, much work remains to be done: "Attempts to build biologically realistic models of cortical circuitry are highlighting how many pieces of the jigsaw are still missing" p. 2190 (10)).

The present study had two immediate goals. One was the scientific goal of mapping how cortical inputs are distributed onto identified postsynaptic pyramidal neurons in monkey temporal association cortex. The second goal was to develop a technical protocol appropriate for long-distance connections, which would improve on standard, electron microscopic (EM) approaches. As a higher through-put EM, we have turned to confocal microscopy, which has been successfully used with double or triple fluorescent markers in several microcircuitry investigations (11-14). Injections of BDA were used to anterogradely label terminations; and a subset of pyramidal neurons, in the anticipated projection focus, was labeled in Golgi-like detail by EGFP, subsequent to infection with a retrogradely transported adenovirus (AdSynEGFP; 15,16 and see Methods for further detail).

Why temporal association cortex? Without doubt, much can be said for focusing instead on primary or early sensory cortices, where the basic connectivity maps are only partially understood, especially in the primate. Our logic, however, has been that enough data exist for these areas, so that fruitful comparisons will be possible. Arguably, data from association cortex is important at this juncture, as a control for whether results from sensory areas can be generalized to other cortices.

The macro-connectivity across the occipito-temporal areas has been extensively investigated at the light microscopic (LM) level (17-28). There is a chain of connections, from areas V4 and TEO, to posterior TE (TEp), and thence to anterior TE (TEa). Of course, there are additionally complex networks of "leapfrog" and reciprocal connections, as well as connectional loops through parts of the superior temporal sulcus and other cortical and subcortical areas. Perirhinal cortex, a multimodal area interconnected with hippocampal CA1, receives dense connections from parts of TE and TEO. The laminar organization of these connections is more complex than for connections between primary and early sensory areas (29, 30). Projections are described as terminating in layer 4 and overlying layer, which would conform to associational or "lateral" connections, in the current

nomenclature, but there is some variability depending on location within a projection focus (core vs. fringe). Retrogradely labeled neurons are in both the supra- and infragranular layers, again generally consistent with associational projections, but with some variability in the proportions (18, 20, 21, 24).

Three brains have been prepared with injections in posterior area TE (TEp). These allow us to investigate the connectional loop: whether and how inputs from TEp contact neurons in anterior area TE (TEa) which project back to the injected zone. In a fourth brain, the injections were placed according to a connectional chain; that is, BDA in TEa labeled projections to perirhinal cortex, and EGFP expressing neurons ("feedforward") were labeled by an injection in more anterior perirhinal cortex (see: Methods 3.7. and Results 4.1. and Figure 1).

Specific questions that we asked are:

1. What happens to "elements of passage" through layer 4 (i.e., apical dendrites from deeper neurons and basal dendrites from neurons in overlying layer 3)? In primary visual cortex, geniculocortical terminations in layer 4 preferentially target spiny stellate neurons; and apical dendrites from deeper neurons are in fact reported to have a diminished spine density as they, a non-preferred target, pass through layer 4 (31). This question broadly addresses the issue of target specificity, especially in the comparison of primary and association cortex.

2. Similarly, in cases where EGFP-expressing neurons occur entirely within a dense termination zone (in layers 1-3, or 1-4), is there preferential targeting of particular dendritic subdomains (ie, basal, apical, oblique, or tuft dendrites)?

3. Do closely neighboring neurons or dendrites have stereotyped, recognizably similar connectivity? An unambiguous answer would be relevant to finer definitions of cortical columnarity.

We stress that this work is part of a broader program toward better understanding of area-to-area communication and connectional interactions across individual, identified neurons. This will evidently be part of a long-term endeavor, and will require a coordinated, multidisciplinary approach, including *in vivo* imaging at cellular, subcellular, and multicellular scales of resolution.

3. MATERIALS AND METHODS

3.1. Animals and Injection sites

Four adult macaque monkeys (*Macaca mulatta*, 4.0-5.8kg) were used in these confocal studies. One additional animal (10 kg) was used for EM only. All animal procedures were carried out in conformity with official Japanese regulations for research on animals, following institutionally approved protocols (RIKEN, Brain Science Institute), and in accordance with the USA National Institutes of Health Guide for the Care and Use of Laboratory Animals (NIH Publication No. 80-23).
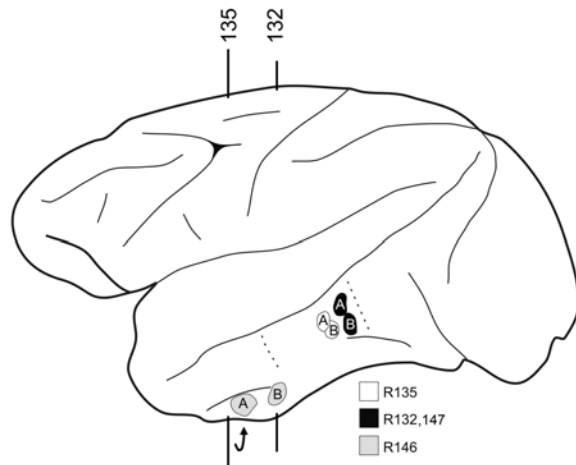
Figure 1. Schematic of a macaque brain left hemisphere, with the location of injection sites indicated from four monkeys. Monkey 147 had an injection of AdSynEGFP (A) in dorsal area TEp, closely overlapping with a similar injection in 132. The other three had injections of AdSynEGFP (A) and BDA (B), as indicated, in dorsal area TEp or (case 146) in more anteriorly. The two sets of interrupted vertical lines correspond indicate the anterior-posterior level of the projection foci selected for confocal analysis in cases 132 and 135 (see also coronal section insets in Figures 4 and 7). The focus in case 146 is located more ventrally (curved arrow, see Figure 9). Dotted lines indicate approximate borders of anterior and posterior TE, and TEO.

Experimental protocols involving AdSynEGFP were approved by the Safety Division of the RIKEN Institute, and were carried out in biosafety level 2 rooms, in accordance with the USA NIH Guidelines for Research Involving Recombinant DNA molecules.

Surgery was carried out under sterile conditions after the animals were deeply anesthetized with Nembutal (35mg/kg i.p., followed by i.v. supplements as needed). Heart rate, EEG, and body temperature were monitored throughout the procedure. A craniotomy was opened over the target area (with reference to 32) and, after incising the dura, location was verified with reference to sulcal landmarks (the superior temporal sulcus, anterior or posterior middle temporal sulci (amts, pmts)). In three monkeys, AdSynEGFP (adenovirus vector, producing EGFP under control of neuron-specific promoter synapsin I) (15, 16) and BDA (Molecular Probes, Eugene, OR) were injected within approximately the same region in posterior TE. In one monkey (146), AdSynEGFP was injected in anterior TE, and AdSynEGFP was injected more anteriorly, in lateral perirhinal cortex (Figure 1). Both tracers were pressure injected through a 10µl Hamilton syringe.

For BDA, a total volume of 2.0 µl was injected in a 10% solution (1:1 mixture of 3,000 and 10,000MW, in 0.0125M phosphate-buffered saline (PBS); pH 7.4). For AdSynEGFP, 1.5µl was injected, at 1.0×10^{12} pfu/ml (15, 16). Two injections of each tracer were made. Injections

were cylindrical, extending through the cortical gray matter, with a short diameter of 1.0-1.5mm.

3.2. Fixation and tissue preparation

After a post-injection survival of 18-22 days, the monkeys were re-anesthetized with ketamine and Nembutal (overdose: 75mg/kg, i.p.), and perfused transcardially, in sequence, with saline containing 0.5% sodium nitrite (for 2 min), 4 L of 4% paraformaldehyde in 0.1M phosphate buffer (PB; pH 7.4; 30 min), and chilled 0.1M PB with 10%, 20%, and 30% sucrose. In two animals (132, 147), small tissue blocks were trimmed postmortem for electron microscopy. In these animals, 0.1% glutaraldehyde was added, and the 30% sucrose buffer was not used. Brains were removed, trimmed, placed in 30% sucrose PB (at 4 degrees C) for 2 days, and then sectioned on a freezing microtome (at 50µm) in a repeating series of 20 sections. In one round, 5 sequential sections were double-reacted for EGFP and BDA by immunoperoxidase, 10 were double-reacted for EGFP and BDA by immunofluorescence, and 5 were reserved for other purposes, for subsequent EGFP-BDA immunofluorescence, or to be discarded,

3.3. Double Immunoperoxidase staining for EGFP and BDA

Sections were washed with 0.1 M PB containing 0.5% Triton-X-100 and reacted with a solution of avidin-biotin complex labeled with horseradish peroxidase (1 drop of reagent per 7 ml of 0.1 M PBS, pH 7.4; ABC Elite kits, Vector, Burlingame, CA), overnight at room temperature. After washes in 0.1 M PB, the sections were reacted with diaminobenzidine (DAB) containing 0.5% nickel ammonium sulfate. This resulted in a black reaction product, corresponding to fibers and terminations anterogradely labeled by BDA. After washing, sections were immunoblocked in blocking solution (0.1 M PBS containing 0.5% Triton-X-100 and 5% normal goat serum, PBS-TG) for 1 hour at room temperature and subsequently incubated with 1 µg/ml of rabbit anti- EGFP antibody (15, 16) in PBS-TG for 2 days at 4 degrees C. Then sections were incubated with biotinylated anti-rabbit secondary antibody (1:200; Vector). To quench residual peroxidase activity of the previous ABC treatment, sections were incubated with 1% H_2O_2 for 5 min. Finally, the biotinylated secondary antibody was visualized by ABC and DAB without nickel ammonium sulfate. Thus, EGFP signal was visualized as brown.

3.4. Double immunofluorescence staining for EGFP and BDA

For confocal analysis, the native EGFP signal was enhanced by immunofluorescence and BDA was visualized using Alexa Fluor 594-conjugated streptavidin (Molecular Probes). Sections were immunoblocked in PBS-TG for 1 hour at room temperature, and subsequently incubated with 10 µg/ml of rabbit anti- EGFP antibody in PBS-TG for 2 days at 4 degrees C. After washing with 0.1 M PBS, the sections were further processed to visualize BDA by fluorescence. For this, sections were incubated for 1.5 hours at room temperature in a mixture of Alexa Fluor 594-conjugated streptavidin (st-avidin, 1:200; Molecular Probes), and secondary antibody Alexa Fluor 488-

conjugated anti-rabbit polyclonal goat antibody (1:200; Molecular Probes).

3.5 Electron microscopy

In two brains, a tissue block was excised for EM analysis. Only one of these (case 281) was used in the present study. The goal was to score synapses onto dendritic shafts, where single neurons had been pre-labeled by AdSynEGFP. The first stage of the protocol was the same as above, except that 0.1% glutaraldehyde was added to the perfusate, and only 10% and 20% sucrose buffers were used. Tissue was vibratome sectioned (at 50μm), and selected sections scanned for EGFP fluorescence. After identifying regions of interest, free-floating tissue sections were processed in primary antibody and blocking solution, with reduced Triton-X (0.01%), anti-EGFP (1μg/ml; overnight at room temperature), followed by anti-rabbit-alexa488, conjugated with nanogold (Invitrogen, Carlsbad, CA; 1:100, 3.5 hrs), and silver enhancement (HQ Silver, Nanoprobes, Yaphank, NY). After scanning by LM, a subset of sections was further processed for EM (osmication, dehydration, and flat embedding in Araldite resin (TAAB, Berkshire, UK). After curing, sections were again scanned by LM and dendrites chosen that were suitable for EM analysis. Areas of interest were trimmed out and glued onto a BEAM capsule. Serial sections were made at 80nm thickness, and observed with a JEOL 1200EX microscope. Micrographs were digitally photographed at 30K magnification.

3.6. Area identification

Several maps have been proposed for the subdivisions of inferotemporal cortex (see 17, 22-29, 32) for recent discussions). In this region, subdivisions can be taken to generally coincide with sulcal landmarks, although the exact boundaries and area terminology have varied according to individual researchers. According to one mapping, which we have adopted, amts designates anterior TE, and pmts approximately designates posterior TE. In addition, the region dorsal to both amts and pmts is distinguished as separate from the ventral region. The region ventral to amts is considered by some as TEav, and the region medial to this, as perirhinal cortex. Some investigators have extended the lateral border of perirhinal cortex further laterally, almost corresponding with area TEav (18, 33). Posterior to area TEp, between pmts and the inferior occipital sulcus, is area TEO.

3.7. Data analysis

Regions where BDA terminations overlapped with EGFP-expressing neurons were identified first in DAB-reacted sections and subsequently in the corresponding fluorescent series. Reference photographs were taken at low magnification (5X or 10X objective), using a Zeiss Axioskop 2 microscope (Carl Zeiss), with the appropriate filter sets for Alexa Fluor 488 (peak excitation, 495nm; peak emission, 519nm) and 594 (peak excitation, 590nm; peak emission, 617nm).

Selected areas of interest were then scanned using the Leica TCS SP2 AOBS confocal microscope

system. Using a 40x objective, z-scanning was performed through the complete thickness of the section (no zoom, frame size of 2048x2048 pixels, pinhole AE = 1.5, pixel size= 183nm; Z-step = 488nm). This medium resolution scan, despite suboptimal settings for pinhole and z-step sizes, was useful for identifying potential BDA-EGFP appositions. The medium resolution z-series was deconvolved using Huygens software (Version 3.0 3p3, Scientific Volume Imaging), and then inspected with the slice viewing capability of the Autoquant Autodeblur software (Version 9.3 Autoquant Imaging Inc). The 3D location of each potential contact was noted for a second, higher magnification scan. Annotation consisted of an arrow to mark the XY location, and a number denoting the Z-step.

Using the 63x objective, higher resolution scanning was performed for each putative contact (zoom = 16, frame size of 256x256 pixels, pinhole AE = 1, voxel size = 58nm, Z-step= 121nm). Location was guided by reference to the medium resolution scan, which was simultaneously displayed on a second computer monitor. High resolution scanning of each putative contact was performed through the thickness of the structure of interest, typically 25-40 Z-steps, or 3-5μm.

Each high resolution z-series was deconvolved using Huygens software, and visualized in the slice viewer of Autodeblur software, as above. At this stage, a proportion of contacts were discarded. Discard criteria were: the visualization of an obvious gap between the bouton and dendritic element; lack of confidence that the putative presynaptic element was in fact a terminal specialization (as opposed to a bend in the axon); poor definition of the dendritic element (e.g., when we could not determine continuity of spines and parent dendritic shaft). After this culling process, the remaining contacts were inspected in 3D with GE Microview software (version 2.1.2 GE Healthcare).

In the final evaluation, contacts were sorted as "high confidence," "low confidence," or "no contact." In high confidence contacts, both the BDA- and EGFP-labeled structures were well-defined, and there was no darkening of pixels visible between the EGFP dendrite and BDA bouton in any of the 3 chosen inspection planes. In low confidence contacts, there was a darkening of pixels at the apposition in 1 or 2 of the inspected slice planes; or the BDA-labeled bouton could not be clearly distinguished from an axon trunk (Figures 2, 3). Axons which traveled predominantly in the Z-plane (AP, since the brains are sectioned in the coronal plane) were particularly hard to resolve with confidence. In the case of doubt on any of these situations, the putative contact was either scored as "low confidence" or discarded.

A point spread function (PSF) was determined using Tetraspek 0.2μm multispectral microspheres (T-7280, Molecular Probes). Confocal z-series of the beads were analyzed with the PSF function in Huygens. This procedure was used to monitor for any misalignment between the different color channels, at an approximately
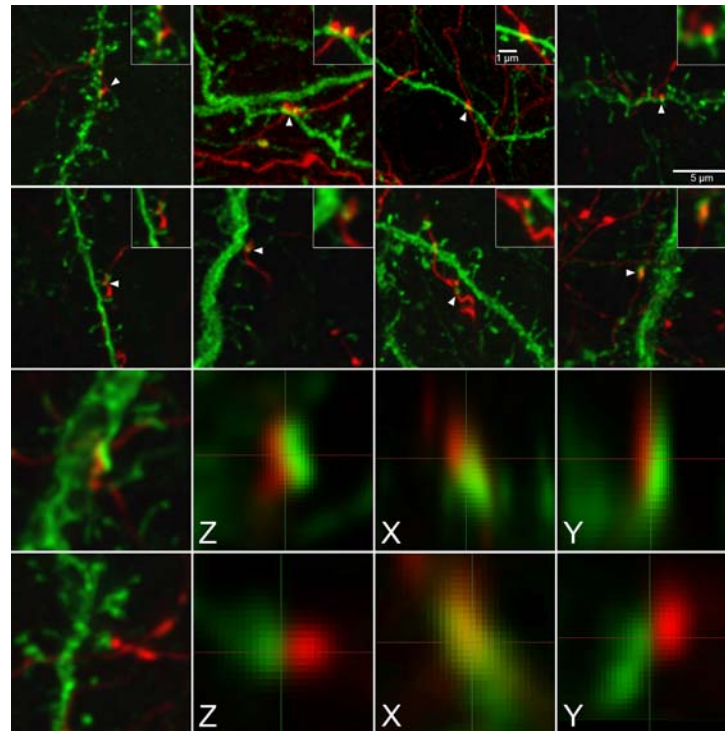
Figure 2. Ten fields of EGFP expressing dendrites (green) and BDA labeled terminations (red). Row 1 across shows four contacts onto dendritic shafts. Contacts (at white arrowheads) are shown at higher magnification in insets, at upper right. Row 2 similarly shows four examples of contacts onto dendritic spines. Row 3 illustrates a shaft contact (maximum projection image, in column 1), and the slice image at three planes of view (columns 2-4). The putative contact is confirmed as such in all three planes. Row 4 illustrates an apparent spine contact (maximum projection image, in column 1), and the slice image at three planes of view (column 2-4). A gap between the spine and bouton is visible in the y and z planes, so that this "contact" would be scored as "low confidence." Scale bars in row 1 apply to all eight images in rows 1 and 2.

monthly time interval. In the unusual case of a detected misalignment, a correcting adjustment was made.

4. RESULTS

4.1. Injection sites

Injections were placed at three sites (Figure 1). In two animals (132 and 135), BDA and AdSynEGFP were injected in area TEpd, toward its posterior border with area TEO. These were intended to reveal a "connectional loop;" that is, do terminations from TEp directly contact reciprocally projecting neurons in area TEa? The third animal (case 147) had injections in the same locus, but EGFP-labeled neurons were used for EM verification of shaft contacts. In a fourth monkey (146), injections were placed more anteriorly and separately. BDA was located in area TEa, just posterior to the amts, and the injection of AdSynEGFP was located anterior and just ventral to amts, in TEav. The projection focus was in the posterior subdivision of perirhinal cortex ("connectional chain"). Terminations from TEad were scored for contacts onto neurons in perirhinal cortex that projected to anterior perirhinal cortex.

4.2. Case 132. connectional loop

We chose a projection focus in the lower bank of the amts (Figure 4). Terminations were mainly in layer 4,

and rather similar to a feedforward projection. Labeled neurons, however, were bistratified, occurring mainly in layer 6 but also scattered through the supragranular layers (18, 21, 24). Some oblique dendrites from ascending apical dendrites were evident in layer 4, but these were relatively few. Neurons located in deep layer 3 extended their basal dendrites well into layer 4.

Abundant apical dendrites of layer 6 neurons were visible as they extended through layer 4 (Figure 5). Because of the sulcal deformation and oblique plane of section relative to the sulcus, apical dendrites were not visualized in continuity with their parent soma, and were predominantly in short segments (<100μm). Thirty-two segments were scanned from both upper and lower layer 4. Of these, 15 received no contacts. Four others received 3 (n=2, 249μm and 314μm segments), 4 (n=1, 64μm segment), or 5 contacts (n=1, 189μm segment); but the majority had 1 (n=6) or 2 (n=5) contacts. No clear pattern emerged in relation to depth location (layer 4a vs. 4b), horizontal location, or segment length (see Table 1).

For comparison, basal dendrites of two deep layer 3 neurons were similarly scanned. For one of these neurons (Figure 6), five dendrites had a total of 8 contacts (1, 2, 5, 0, and 0 contacts). For this neuron, contacts tended to occur in the middle third of the basal dendrite, although at least
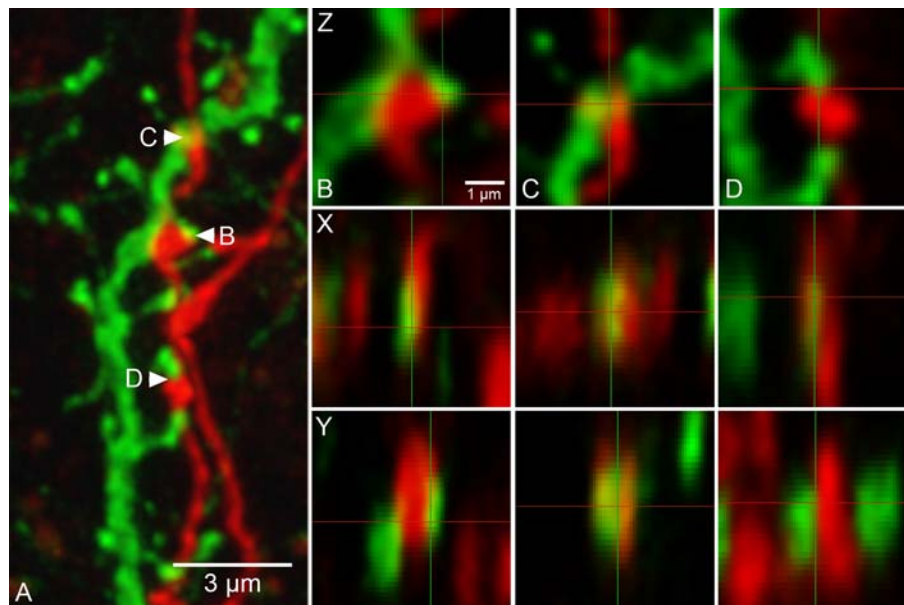
Figure 3. Several BDA-labeled profiles (red) together with an EGFP expressing dendrite (green). A) Three potential contacts are indicated by lettered arrows, and shown at higher magnification in B-D. B) Bouton contacting a spine and shaft. C); bouton contacting a shaft; C) bouton contacting a dendritic spine. Rows 2 and 3 show two additional planes of inspection (x,y) for these three appositions.

Table 1. Case 132. Screening of apical dendritic segments (n=32) from 4 serial sections

| Oblique Dendrite | Potential | 3D | Contacts | | | | | | Length |
| | | | High Confidence Contacts | | | Low Confidence Contacts | | | |
			Spine	Shaft	Total	Spine	Shaft	Total	µm
1	3	1			0		1	1	66
2	1	0			0			0	59
3	2	1	1		1			0	51
4	2	2		1	1	1		1	70
5	2	0			0			0	50
6	2	0			0			0	57
7	3	2	1 (+1?)		2			0	55
8	3	0			0			0	55
9	2	0			0			0	48
10	3	0			0			0	52
11	6	5	1	3	4		1	1	63
12	2	2			0	(1B?)	(1B?)	2	56
13	1	1	(+1?)		1			0	71
14	1	0			0			0	66
15	2	0			0			0	55
16	1	0			0			0	59
17	6	3		2	2		(1B?)	1	187
18	0				0			0	66
19	2	0			0			0	51
20	2	1			0		(1B?)	1	145
21	3	3		1	1	1	1	2	77
22	7	4	1	1	2	1	1	2	225
23	1	0			0			0	176
24	6	6		3	3	(1B?)	2	3	249
25	7	5	1	2	3		1	1	214
26	3	3	1	1	2	(+1?)		1	187
27	2	2	2		2			0	184
28	1	0			0			0	192
29	6	5	1	4	5			0	189
30	7	2	1		1	(1B?)		1	211
31	2	2			0	1	1	2	186
32	2	2	1		1			0	207

one far distal contact was found. Some branches were devoid of contacts; and within a dendritic branch, not all segments had contacts. A similar result was obtained for a second cell, where 5 basal dendrites had a total of 1, 6, 3, 3, and 1 contact, respectively. For this and almost all other neurons, however, serial reconstructions were not
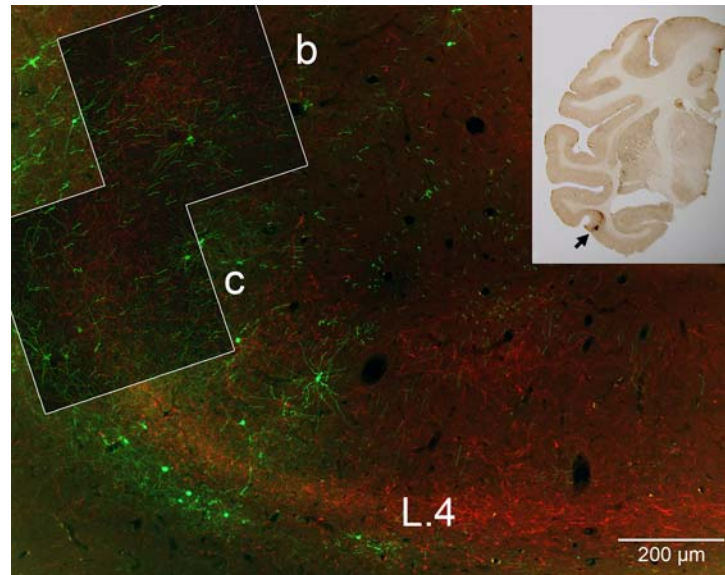
Figure 4. expressing neurons, mainly in layer 6. There are also scattered neurons in the supragranular layers. Inset (inverted in relation to the micrograph): closely adjacent coronal section, reacted with DAB, to show the location of the projection focus (arrow). The squares (b,c,) designate subregions analyzed by confocal microscopy. The dendrites and neuron in figures 5 and 6 are from a closely adjacent field.
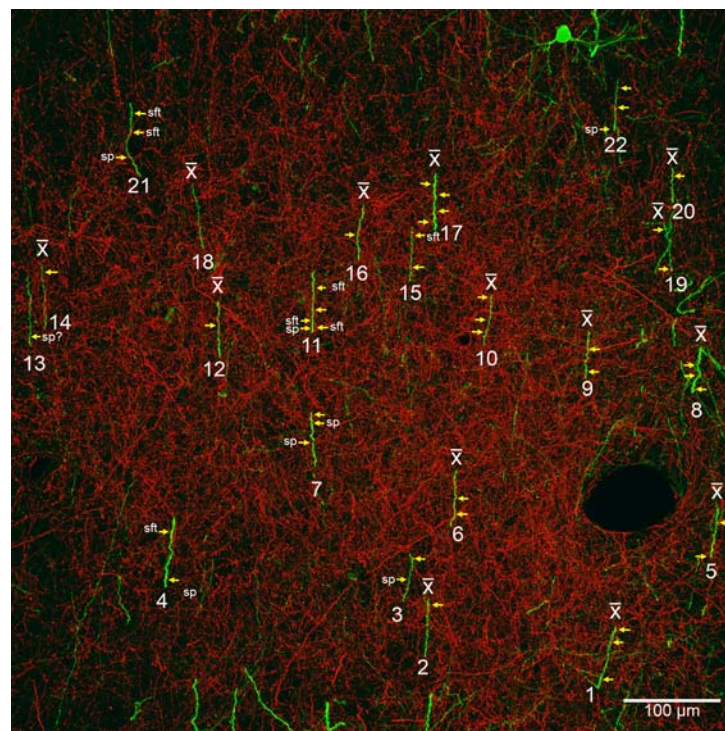

Figure 5. Dense BDA-labeled terminations (red; case 132) in layer 4, with apical dendritic segments (green) from neurons in layer 6 (case 132). These are reciprocating connections between areas TEpd and TEad. Potential contacts (unlabeled arrows) were first identified at medium (40X objective) and high resolution (63X objective), and subsequently verified by inspection in three planes of view. 3-D verified contacts are designated by labeled arrows (sp=spine; sft=shaft). For clarity, an "x" marks segments for which none of the potential contacts could be considered as verified. Individual dendritic segments are numbered (and see Table 1).
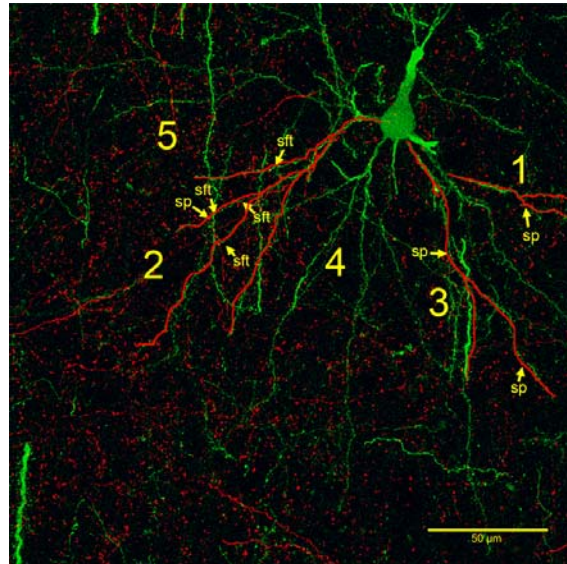
Figure 6. EGFP-expressing neuron in deep layer 3, with basal dendrites extending into layer 4 (case 132). Three spine contacts occur on dendrites 1 and 3, no contacts on two of the dendrites (4 and 5), and five shaft contacts on dendrites 2. Only 3-D verified contacts are shown. The neuron was not followed in adjacent sections, and distal dendritic portions can be assumed to be incomplete. The three dendrites with contacts are shown in red. Dashes and L. 4 = layer 4.
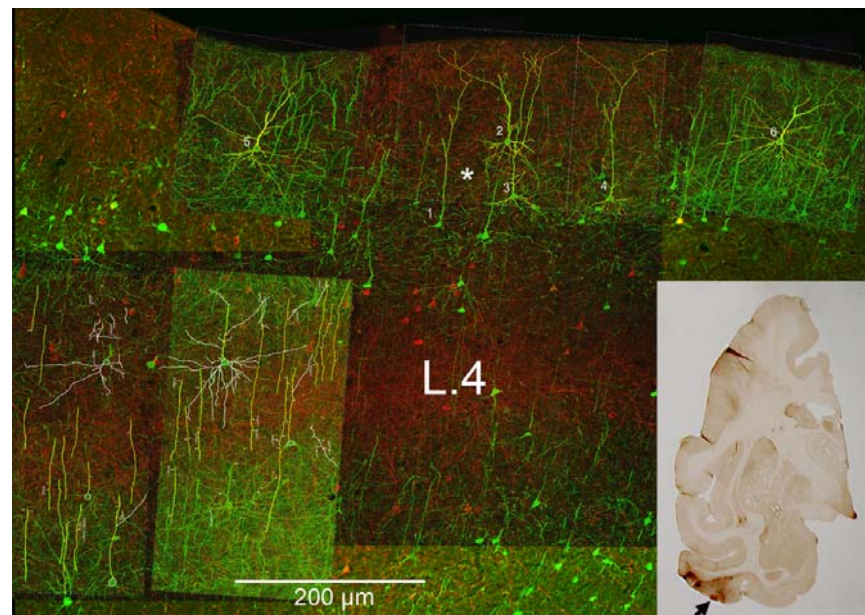

Figure 7. Fluorescent micrograph (case 135) of BDA labeled terminations in layer 4 and upper layers of area TEad. EGFP-expressing neurons are evident in layers 5, 3 and 2. Inset (rotated in relation to micrograph): closely adjacent coronal section, reacted with DAB, to show the location of the projection focus (arrow). Region at the asterisk is shown at higher magnification in Figure 8.

undertaken. Therefore, data are only semi-quantitative and, as concerns bouton distribution in particular, should be interpreted with some caution.

4.3. Case 135. connectional loop

The projection focus was slightly dorsal and posterior to that in case 132, located within area TEad on the lateral surface (Figure 7). Terminations again were concentrated in layer 4, but extended further into layers 1-3 (as in ref.). The pattern of retrograde labeling was also slightly different, with more involvement of layer 5 (both 5a and 5b) instead of layer 6. Basal dendrites of deep layer 3 neurons extended into layer 4. The laminar signature conforms more closely to an associational projection,

probably because the injections were less posterior than in case 132.

Apical dendrites of layer 5 neurons were abundant in layer 4. Because of a more favorable plane of section, apical segments were on average considerably longer than in case 132 (range: 100-439μm), with only three shorter segments (59, 65, 68μm). Continuity with parent neurons in layer 5a could often be established. Despite the longer lengths, 44 of 62 segments had no contacts, and only 18 had 1 (n=14) or 2 contacts (n=4). No pattern could be ascertained between number of contacts and laminar depth or segment length. For example, segments with 2 contacts measured 148, 178, 197, and 217μm; but segments with no contacts were as long or longer (Table 2).

With the idea that contacts might prefer oblique branches, we scanned 22 oblique segments (96-645μm; Table 3). Of these, the majority (n=16) had no contacts, and only 6 had 2 (n=2; 520 and 594μm segments) or 1 contact (n=4; 152, 328, 372, 645μm segments). Only a small number of oblique dendrites were evident from the apical dendrites passing through layer 4.

Basal dendrites of two deep layer 3 neurons were scanned in layer 4; but only one spine contact was found. From these results, we can suggest that basal dendrites, ascending apical dendrites, and oblique dendrites are only infrequently contacted by these cortical terminations in layer 4; and comparison of these two cases indicates that ascending dendrites of layer 5 neurons are less frequently contacted than those of layer 6 neurons.

Since dense BDA label in this case extended through layers 1-3, we also analyzed ten neurons located more superficially, in layers 2 and 3a. These single neurons, although not reconstructed in full, provided information about possible target preference within a single neurons or according to laminar depth. As shown in Table 4, this sample showed a wide range of contact number. Two cells (cells 3, 4) had 1 contact, one cell (cell 1) had no contacts, and one cell (cell 6) had 3 contacts. Cells 1 and 4 are obviously incomplete, but cells 3 and 6 are less so.

Of the remaining six cells, two (cells 2 and 10) were exceptional for a comparatively large number of contacts (nineteen for cell 2; fifteen for cell 10). Cell 2 had a relatively superficial location, in contrast with cells 1, 3, and 4; but cell 10, with the second highest contact number, was situated in a deeper stratum. Cells 5 and 7, both with intermediate contact numbers (8 and 6) were located about at the same level as cell 2. From these data, we suggest that neighboring neurons can have widely different contact numbers.

For cell 2, with the highest contact number, contacts were distributed without any clear preference for dendritic compartment (5 contacts on basal dendrites, 5 on apical dendrite, and 9 on the apical tuft; Figure 8). Cell 10 had a similar distribution onto basal dendrites (4 contacts), apical obliques (6 contacts), and apical tuft (5 contacts).

For basal dendrites, contacts in cell 2 appeared to prefer the middle one-third (Figure 8A), but those on cell 10 occurred both at a distal tip as well as more proximally.

4.4. Case 146. connectional chain

The projection focus was in perirhinal cortex (Figure 9). Cortical terminations, labeled by a BDA injection at the border of areas TEa and TEp (Figure 1), were concentrated in layer 4, but extended into the overlying layers 1-3. Neurons were densely labeled by a more anteriorly placed injection, just ventral to amts, and were located in layer 5 (5a and 5b) as well as in the supragranular layers. The injections of BDA and AdSynEGFP were more widely dissociated in this animal. BDA labeled terminations are thus part of a "connectional chain," as opposed to the "connectional loops" in the previous two cases.

As in case 135, apical dendrites passing through layer 4 were in long segments (Figure 9) and frequently in continuity with parent cells in layer 5a. Of 37 segments analyzed (116-382μm), 24 had no contacts in layer 4. The remaining 13 had 1 (n=8), 2 (n=3), or 4 contacts (n=2). As for the previous two cases, contacts occurred on shafts as well as spines and, in the case of multiple contacts, were spaced rather than clustered (Figure 10A). Also as for the previous two cases, oblique dendrites off the apical had only a few or no contacts, but there were overall few oblique dendrites in layer 4.

Basal dendrites of fifteen deep layer 3 neurons were analyzed in layer 4. Of these, 8 had no contacts, and the remaining 7 had only a few (3 cells=1 contact, 2 cells = 2 contacts, 1 cell = 3 contacts, and 1 cell = 4 contacts).

Distal tufts from 10 neurons in layer 3 were scanned in layers 1 and 2 (Figure 10B). In contrast with case 135 (neurons in area TEad), these had relatively few contacts (1 tuft = 0 contacts, 3 tufts= 1 contact, 2 tufts = 2 contacts, 1 = 3 contacts, 2 = 4 contacts, and 1 = 6 contacts). Contact number was too small to allow any conclusions about distribution preference within the tuft. However, we remark that there was no evidence for clustered contacts, and no evident preference for distal most locations in layer 1a.

4.5. Spine density

Spine density is known to vary over different parts of the dendritic tree (35). In a small sample, we counted spine density (Table 5) along 16-43uμ segments from apical dendrites in layer 4 (n=2 from case 146; n=2 from case 132) and, in layer 3 (case 147), from basal dendrites (n= 5 distal; n= 5 middle portion); apical dendrite (n=2, about 75-100μm from the soma), oblique dendrites (n=2), and distal tuft (n=2). Inter-spine interval ranged from 0.3μm (for an apical dendrite) to 1.5μm (from a mid-portion basal dendrite in layer 3). There was some tendency for distal basal dendrites to have a lower density, but this was only slight (Figure 11 and Table 5). The main apical shaft, with higher spine density, was also thicker in diameter. So far, in our material, there is no obvious relationship between target preference and spine density.

Confocally mapped inputs onto identified pyramidal neurons

Table 2. Case 135. Screening of apical dendritic segments (n=63) from 3 serial sections (88-90)

				Contacts						Length
				High Confidence Contacts			Low Confidence Contacts			
AD	Sect.	Potential	3D	Spine	Shaft	Total	Spine	Shaft	Total	μm
				Spine	Shaft	Total	Spine	Shaft	Total	μm
1	90	3	3		1	1		1	1	240
2	90	4	1		1	1				154
3	90	4	2							191
4	90	4	2		1	1	(1B?)		1	178
5	90	3	0							238
6	90	7	3					1 (1B?)	2	439
7	90	2	0							281
8	90	3	0							239
9	90	2	1							214
10	90	3	1		1	1				168
11	90	4	2		2	2				217
12	90	3	0							310
13	90	3	0							215
14	90	0	0							118
15	90	3	0							133
16	90	1	0							122
17	90	3	2		1	1		1	1	135
18	90	1	0							149
19	90	2	0							235
20	90	1	0							143
21	90	2	0							129
22	90	1	0							144
23	90	0	0							119
24	90	3	1		1	1				108
25	90	4	1	1		1				143
26	90	5	1	1		1				81
27	90	2	0							100
28	90	5	1					1	1	110
29	90	2	0							106
30	89	1	0							224
31	89	2	1				(1?)		1	176
32	89	1	1		1	1				242
33	89	1	0							160
34	89	0	0							211
35	89	5	1				(1?)		1	347
36	89	3	2					1	1	331
37	89	0	0							121
38	89	5	2	1	1	2				197
39	89	2	2				1 (1B?)		2	180
40	89	1	0							129
41	89	1	0							186
42	89	2	1	1		1				185
43	89	0	0							68
44	89	0	0							109
45	89	3	3	1	1	2		1	1	148
46	89	1	0							156
47	89	0	0							142
48	89	1	0							191
49	89	2	1	1		1				157
50	89	1	0							102
51	89	0	0							127
52	89	0	0							112
53	89	3	0							155
54	89	1	0							117
55	88	7	0							205
56	88	4	0							151
57	88	12	2	1	1	2				278
58	88	15	1		1	1				287
59	88	1	1		1	1				65
60	88	6	0							59
61	88	1	1		1	1				120
62	88	10	0	1						174
63	88	3	0							183

4.6. BDA density

The number of contacts in our material was highly variable, even for neighboring neurons or dendritic segments. Thus, we have some confidence in discounting he possible influence of bouton density. That is, could a higher number of contacts simply reflect a denser field of terminations? In addition, in comparing fields of high density terminations in cases 132 and 135, it was obvious

Confocally mapped inputs onto identified pyramidal neurons

Table 3. Case 135. Screening of oblique dendritic segments (n=22)

Oblique Dendrite	Potential	3D	Contacts	Length	Oblique Dendrite	Potential	3D	Contacts	Length
			High Confidence Contacts	Low Confidence Contacts				High Confidence Contacts	Low Confidence Contacts
			Spine	Shaft				Spine	Shaft
1	2	0			1	2	0		
2	0	0			2	0	0		
3	3	1			3	3	1		
4	5	2			4	5	2		
5	1	1		1	5	1	1		1
6	2	0			6	2	0		
7	6	2		1	7	6	2		1
8	2	1			8	2	1		
9	5	2			9	5	2		
10	1	0			10	1	0		
11	2	0			11	2	0		
12	4	2		1	12	4	2		1
13	2	0			13	2	0		
14	3	0			14	3	0		
15	7	2			15	7	2		
16	3	0			16	3	0		
17	3	0			17	3	0		
18	2	2			18	2	2		
19	4	1			19	4	1		
20	8	3		2	20	8	3		2

Table 4. Case 135. Screening of neurons (n=10) in layers 2 and upper 3

Cell	Potential	CONTACTS						Depth	BDA
		High Confidence Contacts			Low Confidence Contacts				
		Spine	Shaft	Total	Spine	Shaft	Total	μm	
1	7			0	(1B?)	(1B?)	0	405	high
2	91	11	8	19	7 (2B?)	7 (3B?)	19	220	high
3	14	0	1	1	1	1 (2B?)	4	340	high
4	6	1		1		1	1	335	med
5	23	4	3	7	1		1	220	med
6	12	2	1	3	1 (1B?)	1	3	190	low
7	27	3	3	6			0	200	med
8	36	6	3	9	1 (1B?)	1 (1B?)	4	220	high
9	52	4 (+1?)	6	11	3 (1B?)	1 (2B?)	8	255	high
10	61	3	12	15	1 (1B? +1?)	3 (1B?)	7	320	high

Table 5. Dendritic spine counts for 18 segments

Segment	No. of spines	Segment length (μm)	Inter-spine Interval (μm)
Basal 1 distal	35	32	0.9
Basal 1 middle	24	35	1.5
Basal 2 distal	34	41	1.2
Basal 3 distal	45	39	0.9
Basal 3 middle	36	32	0.9
Basal 4 distal	27	31	1.1
Basal 4 middle	38	32	0.8
Basal 5 distal	53	43	0.8
Basal 5 middle	39	34	0.9
Apical Dendrite (cell1)	61	16	0.3
Apical Dendrite (2)	51	22	0.4
Basal middle (cell1)	41	35	0.9
Basal middle (cell1)	49	40	0.8
Mid Tuft (cell1)	28	32	1.1
Mid Tuft (cell1)	46	37	0.8
Distal Tuft (cell1)	36	30	0.8
Distal Tuft (cell1)	37	30	0.8
Apical Dendrite 1 (L.4)	72	34	0.5
Apical Dendrite 2 (L.4)	68	32	0.5
Apical Dendrite 1 (L.4)	98	35	0.4
Apical Dendrite 2 (L.4)	88	32	0.4

by visual inspection that the density was greater in 135 (Figure 12). Despite that, the proportion of contacts, measured for apical dendritic segments in layer 4, was actually less in 135.

Boutons are known to occur as beads (boutons en passant) or stalked (spinous) profiles (boutons terminaux). In confirmation of a previous report (36), we easily found all combinations of shapes: beaded boutons contacting
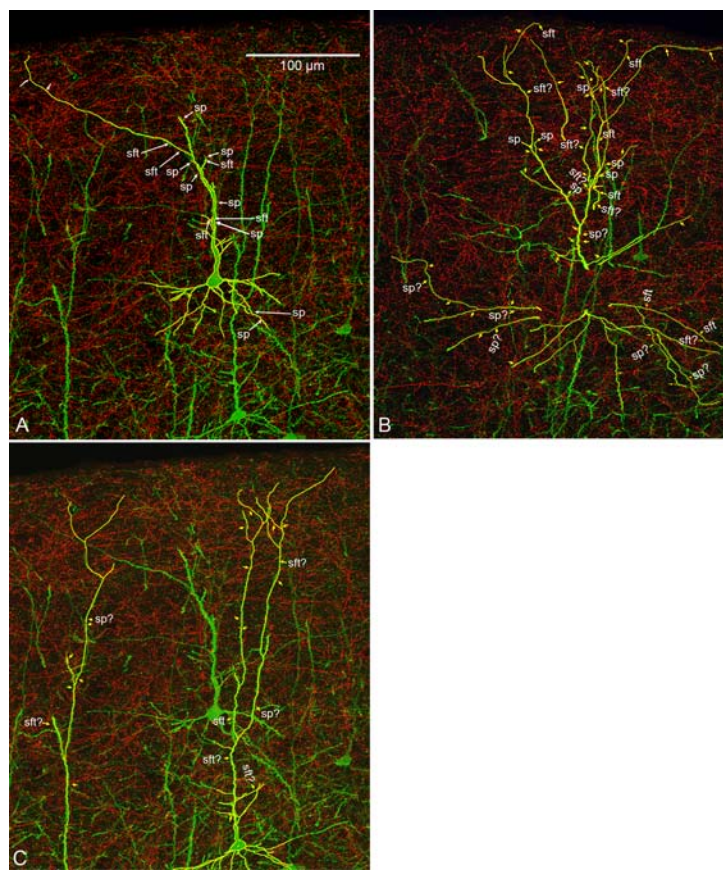
Figure 8. Three fields of EGFP-expressing neurons in layers 2 or upper 3. 3-D verified contacts are shown as labeled arrows (see also Table 2). A) and C) are from the region to the right (A) or left (C) of the asterisk, in figure 7. The neuron in B) is from a similar region in a closely adjacent section. Neurons are not reconstructed through serial sections and are incomplete to varying degrees.
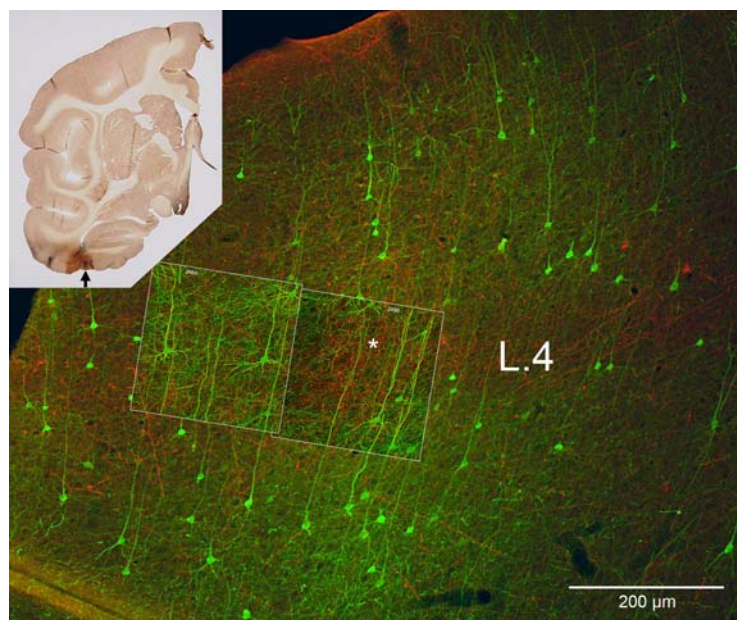

Figure 9. Fluorescent micrograph (case 146) of BDA labeled terminations in layer 4 and upper layers of perirhinal cortex. EGFP-expressing neurons are evident in layer 5 and scattered in layers 2 and 3. Inset (rotated in relation to the micrograph): closely adjacent coronal section, reacted with DAB, to show the location of the projection focus (arrow). The region from the asterisk is illustrated in a confocal projection image in figure 10.
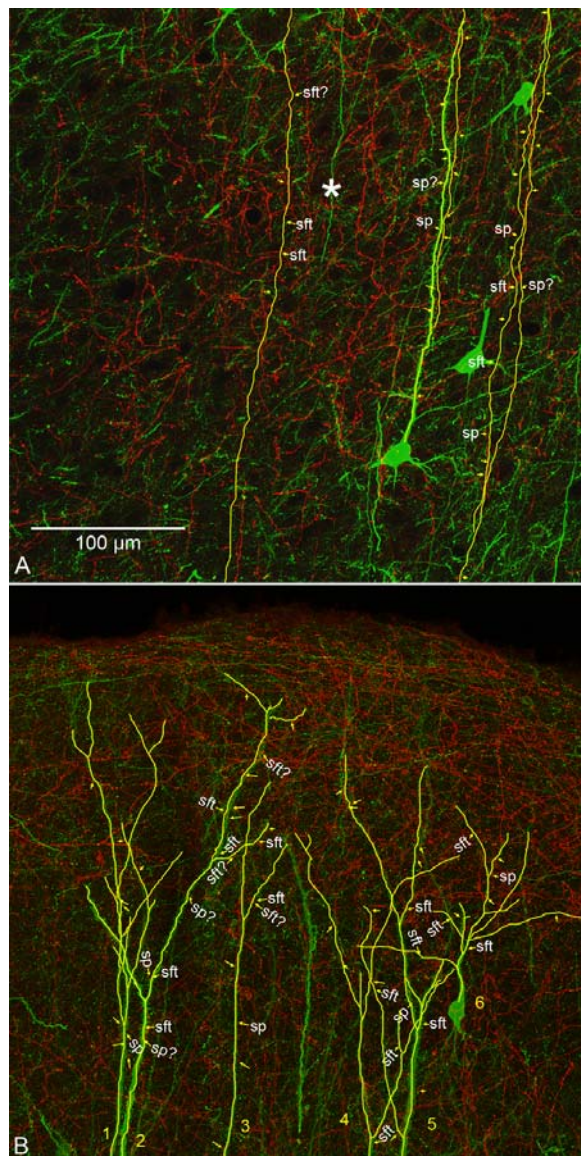
Figure 10. A) A field of long apical dendritic segments, from neurons in the deeper layers, passing through a zone of BDA labeled terminations in layer 4 (see figure 9). B) A field of five distal apical tufts from neurons in upper layer 3, and one neuron in layer 2 (neuron 6). 3-D verified contacts are shown as labeled arrows.

dendritic spines, and also shafts; and stalked terminations contacting dendritic shafts and also spines.

4.7. Apical dendritic contacts, in EM

To further investigate the distribution of excitatory synapses on dendritic shafts of pyramidal neurons, we carried out EM analysis in one brain (case 281). EGFP-expressing neurons were produced in area TEp by injecting AdSynEGFP in a more posterior region of area TEp (thus, producing lateral or intrinsic connections). For histological processing, EGFP signal was visualized by using anti-EGFP antibody and secondary antibody

conjugated with alexa-488 nanogold. This was followed by silver enhancement (see Methods 3.5.). Silver enhancement was used as an alternative to DAB, for the sake of better visualization of any postsynaptic density. In this tissue, only AdSynEGFP was used, as a single label. Synapses were scored by standard criteria (vesicle shape, and presence or absence of postsynaptic density), but they were not labeled with BDA.

A portion of apical dendrite was selected from a pyramidal neuron in layer 5b, and 80nm serial sections were obtained from a 20μm segment in layer 5a (Figure 13). Over a 17μm extent, we identified 18 synaptic contacts. Of these 3 were clearly asymmetrical, and 6 were symmetrical. We identified nine others as symmetrical, but with lower confidence. This ratio, of 3: 15, or 16% is in range with most reports in the literature (7, 8, 35), but less than for our confocal material, where shaft contacts appear as relatively abundant. We are supposing that some, and presumably many, of the shaft contacts in our material are actually onto closely neighboring, but unlabeled spines.

5. DISCUSSION

In the next generation of connectivity studies, microcircuitry is likely to advance at an increasingly rapid pace. Confocal microscopy, in some variant of the experimental design presented here, can be a very useful way of achieving necessary baseline data. Although the long-term goals of elucidating synaptic efficacy and connectional interactions will require more dynamic, physiological approaches, it nevertheless should be possible to obtain input maps for specific cell populations, and to correlate these with further subtype characteristics. In this discussion section, we summarize first, some of the technical factors of this approach, and then some of our main microcircuitry results.

5.1. Technical considerations

Confocal microscopy has obvious advantages of resolution over conventional light microscopy and, with appropriate software, can provide reasonably confident assessment of whether a bouton is actually in physical contact with a potential postsynaptic element (12-14). Compared with EM, it allows easier switching between low and high magnifications, as is important to achieve both global orientation and higher resolution. Analysis is faster than with EM, the tissue preparation steps are easier, and the necessity of high quality ultramicrotomy is eliminated. These are all obvious advantages. Nevertheless, it is important to point out several significant limitations.

A major problem concerns not the confocal analysis itself, but rather what can be achieved with present methods of labeling for pyramidal cells and their afferent inputs. In mice, the generation of transgenic lines or electroporation of GFP can routinely demonstrate large neuronal populations. For the monkey, and especially for pyramidal cells, most methods are limited to visualization of soma and proximal dendrites. These do not necessarily label dendritic spines; yet spines are the primary postsynaptic target for excitatory inputs. The AdSynEGFP
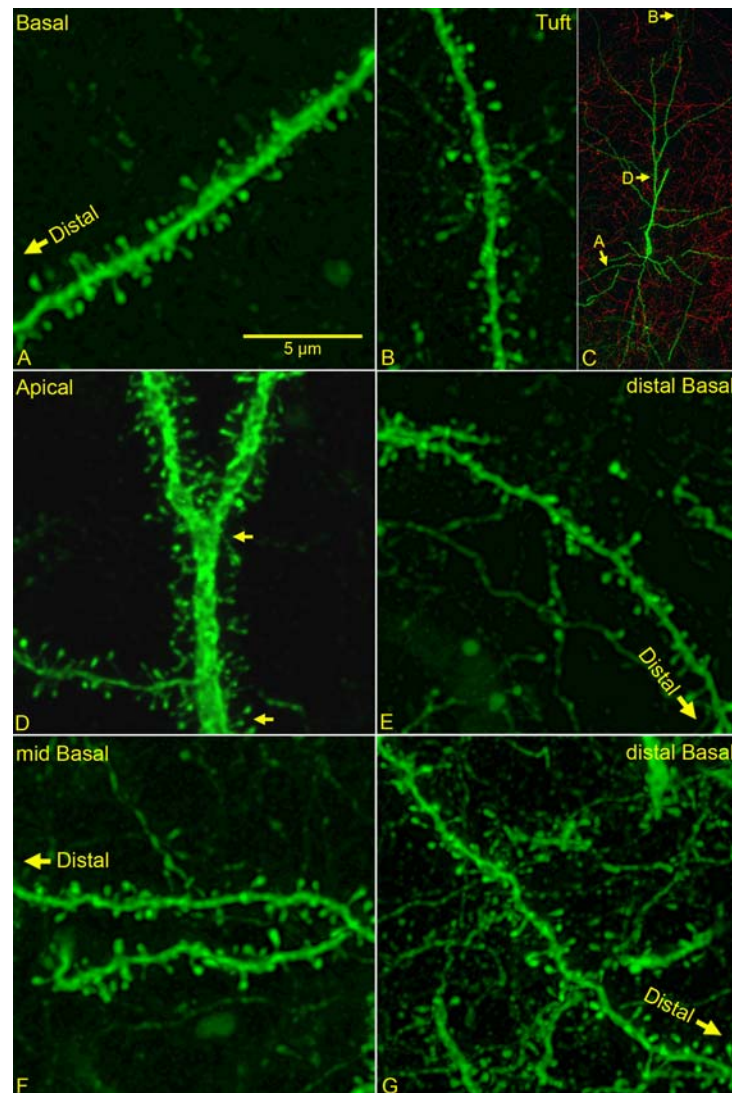
Figure 11. Confocal maximum projection images from six different segments of EGFP-expressing neurons, to illustrate spine detail and density. A), B), and D) are from the same neuron, and sampled regions are indicated by corresponding letters in C). The arrows in D) bracket the portion used for spine counts. E- G): Distal or middle portions from three other basal dendrites.

used here appears to be reliable, in comparison with standard retrograde tracers, and superior in that Golgi-like detail is routinely produced. Other viral vectors are fast becoming available (37-39). Since, however, these techniques rely on *in vivo* injection, only the subset of pyramidal neurons that are projecting to the injection site are labeled. The small pyramids in layer 4 are not labeled, and multiple other efferent populations will not be labeled unless multiple injections are made. This can be done, with some effort, but, unless multiple colors are available ("rainbow AdSyn"), the different populations will not be identifiable.

The population of BDA-labeled terminations is also subtotal, deriving only from projection neurons within the effective uptake zone of the injection site. Other neurons from the same cortical area, but outside the immediate injection site, certainly contribute convergent

terminations to the same focus, but these will not be detected. Furthermore, extracellular injections, necessary to achieve dense terminations, mask the exact parent neuron and even the identity of its home layer.

The need for separate injections of BDA and AdSynEGFP makes for same difficulty in achieving an optimal overlap zone where there is both dense input and abundant neuronal labeling. In our experience, a satisfactory degree of overlap can be achieved with multiple injections of both BDA and AdSynEGFP; but for any projection focus, the two labels may in part be offset, side-by-side, as a consequence of the topographic geometry of the injection sites. Even in the case of adequate overlap, the density of BDA-labeled terminations will vary, and careful account needs to be taken of this variability. That is, does an apparently greater number of contacts simply reflect a greater density of terminations, as opposed to any
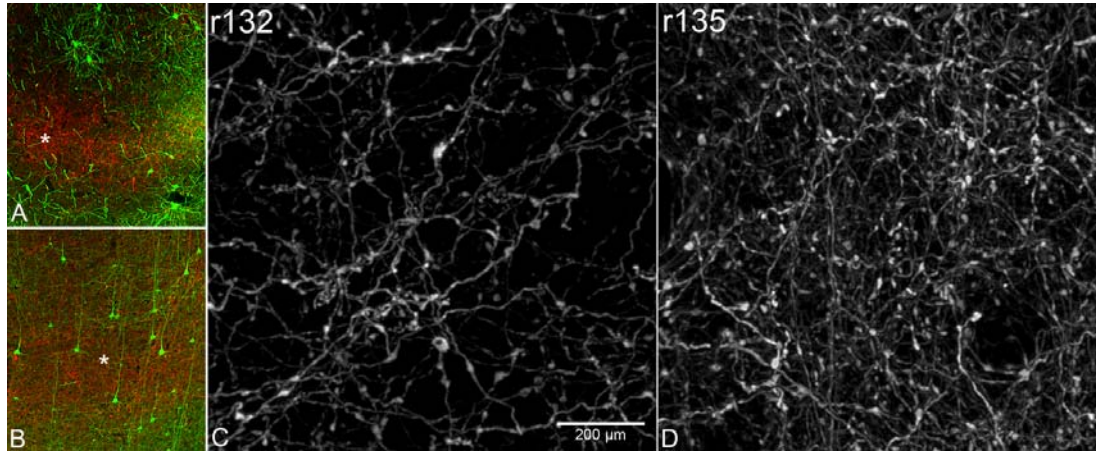
Figure 12. Density of BDA labeled terminations. A), B) Low magnification fluorescent micrographs of BDA labeled terminations and EGFP-expressing neurons, from cases 132 (A) and 135 (B). The asterisks indicate what appears to be zones of densest terminations. These were scanned by confocal (63X objective), and compared qualitatively. The boutons appear slightly less dense in case 132 (C) than case 135 (D). The number of dendrites with contacts was higher, however, in case 132 (compare Tables 1 and 2).

target specificity? This can be controlled for by comparing number of putative contacts with density measurements. In our material, however, we have relied on qualitative analysis and trends which seemed to discount the influence of background density. First, the number of contacts clearly varied for neighboring profiles, regardless of whether these are both in a zone of high or low density termination. Second, the proportion of neurons with contacts was actually reversed in relation to background density; namely, case 132 had a higher proportion (50%) of apical segments with contacts than case 135 (30%), but the BDA density was lower in case 132 (Figure 12).

As concerns the confocal analysis proper, a major issue is the confident assessment that a terminal is in fact in direct physical contact with a postsynaptic target and, further, that this can be assumed to be a synapse (14). One approach to this problem is to use a synaptic marker, such as antibodies against synaptophysin; but in our experience, tissue penetration has not been satisfactory in primate material (see also 11). Accordingly, in this study, our verification of putative contacts has been by inspection, aided by 3-D software. As a result, our actual scores can be regarded as a small subset of potential contacts (less than if we included contacts scored as "low confidence").

The verification of contacts as actual synapses is of major importance. If the contacts scored as "low confidence" are included, the contact numbers are significantly higher (see Tables 1-4). How to treat this issue is still under debate. On the one hand, some degree of structural turnover and remodeling, for both dendrites and axons, is now well documented in primary sensory areas (40-46). Given this, one can argue that potential pre- and postsynaptic contacts that are in very close proximity should be in fact considered as "potential contacts." On the other hand, we have been concerned that more data are still needed about the frequency of

axonal and dendritic remodeling in different species and areas. This concern is reinforced by various "anomalous" results, such as the large number of contacts onto pyramidal dendritic shafts. This is unusually large, according to other reports in the literature (35); and we have supposed that many of these are actually contacts onto other, non-labeled spines in close vicinity to the apparent shaft contact. Preliminary EM analysis of shaft contacts onto an apical dendrite in area TEp is consistent with the lower number from the literature (Figure 13 and Results 4.7.). In the next phase of this project, we plan to use selective EM verification in order to establish baseline confidence level for the confocal contacts; for example, a sample of 20 confocal contacts that are subsequently verified by EM as actual synapses.

5.2 Microcircuitry considerations
5.2.1. Layer 4

The three brains used for combined BDA and EGFP had several different potential postsynaptic populations in layer 4: apical dendrites of layer 6 neurons (case 132) and apical dendrites of layer 5 neurons (case 135), both of which project back to the injection site; apical dendrites of layer 5 neurons (case 146) which project to an anterior injection site ("feedforward" or "lateral"); basal dendrites of deep layer 3 neurons which project back to the injection site (case 132, 135), and basal dendrites of layer 3 neurons which project to an anterior injection site (case 146). Of these, about 50% of the layer 6 dendritic segments received contacts in layer 4, but only 30% (case 135) and 35% (case 146) of the layer 5 apical dendrites. Basal dendrites in case 146 ("feedforward") had few or no (8 of 15 cells) contacts, those in case 135 had few contacts, and those in case 132 slightly more, although still overall few. From this, we conclude that the main target of cortical terminations in layer 4 may be the small, intrinsically projecting pyramidal neurons (Figure 14). This would be consistent with the "relay" role of layer 4, as understood from primary sensory areas (1, 29, 35). We note, however, is that in layer
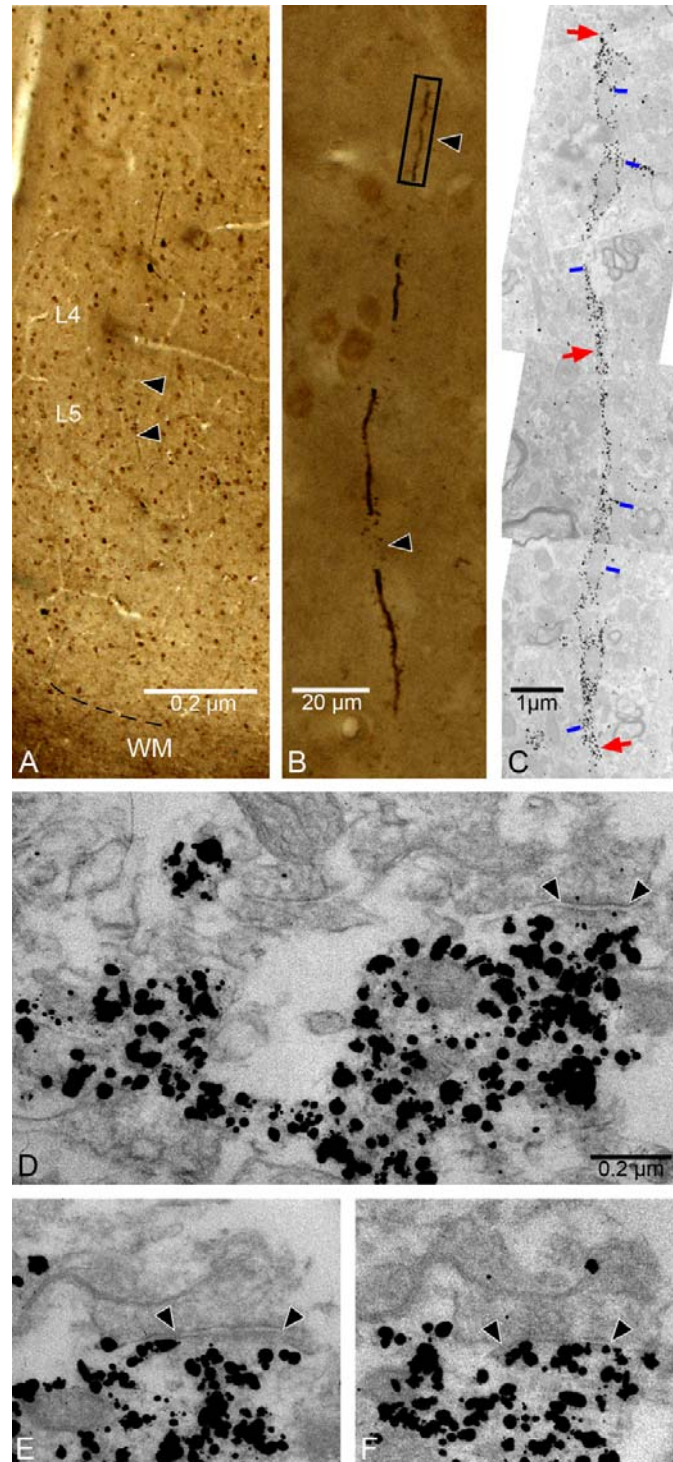
Figure 13. A) Resin embedded flat section from area TEpd (case 281). EGFP expressing segments have been visualized with silver-enhanced nanogold. The portion between the arrowheads, at the border of layers 4 and 5, is shown at higher magnification in B). B) The dendritic segment demarcated by arrowheads corresponds to the segment between arrowheads in A). The framed segment was serially sectioned for EM. C) Low magnification montage of the same dendritic segment. Red arrows indicate the position of three asymmetric shaft synapses. Blue bars indicate a subset of clearly identified spines. D-F) Serial sections of an asymmetric synapse (between the arrowheads) onto the dendritic shaft. Postsynaptic density is visible in D) and E), and synaptic vesicles in F). The black dots correspond to silver-enhanced nanogold.
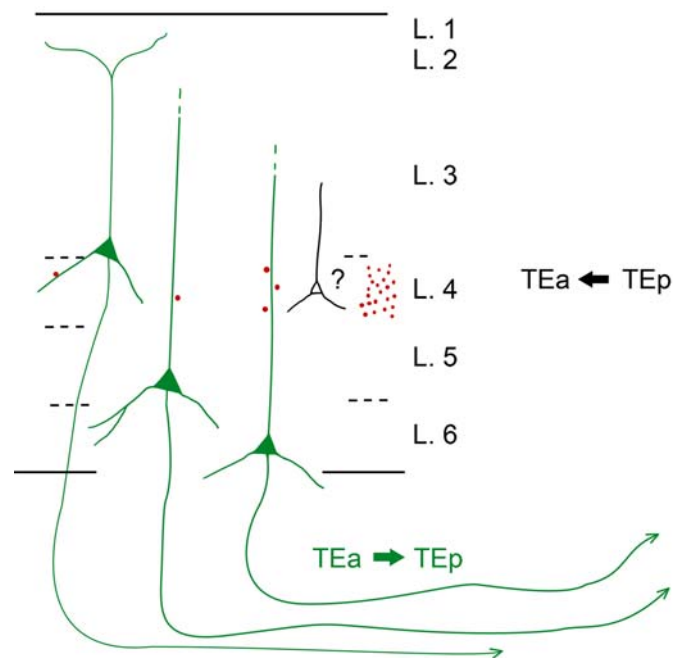
Figure 14. Cortical terminations in layer 4 show target selectivity. That is, for apical dendrites of layer 6 neurons, about 50% receive contacts, and contacts are commonly multiple. However, for apical dendrites of layer 5 neurons, only about 30-35% receive contacts, and the number of contacts is only 1-2. Similarly, basal dendrites of deep layer 3 neurons receive only a few contacts. We suggest that the main targets are 1) intrinsic neurons in layer 4 (?), and/or 2) dendrites of neurons in layer 3, 5, or 6 that do not project back to the injected area. Both these possibilities would imply a preference for polysynaptic processing, as opposed to direct, monosynaptic reciprocal loops. In this example, we have illustrated feedforward terminations from TEp to layer 4 of TEa, and neurons in TEa, projecting back to TEp.

4 of association cortex there is no apparent diminishment in density of dendritic spines belonging to the apical dendrites.

An alternate interpretation of these results is that cortical input may preferentially target elements in layer 4 that were not labeled in our material; that is, dendrites belonging to neurons projecting subcortically or to other cortical areas that we did not inject.

Differential connectivity for apical dendrites of layer 6 vs. layer 5 neurons may indicate that the degree of direct reciprocal connectivity is connectionally dependent and, in the case of corticocortical connections, is greater for layer 6 neurons. This supports the idea of a special role for layer 6; that is, both as a "higher order" layer with integrative properties and as a primary input layer, conveying interlaminar excitation (47).We also found that basal dendrites of layer 3 projection neurons receive relatively few contacts; but this requires further confirmation.

5.2.2. Variability

From all three brains, our results support the interpretation that closely neighboring cells dendrites do not share any obviously stereotyped, common connectivity (48, 49). This is most apparent for the long apical dendritic segments in case 135 and case 146, where some segments

have contacts and others not, but according to no discernible spatial distribution. A similar variability occurs also in the set of 10 superficial neurons in case 135. Two possible interpretations are: 1) the connectivity is "random" or 2) there is selectivity, but according an unknown rule; for example, there could be subtype diversity among the labeled pyramidal cells (6-8, 50). Our pyramidal cell population all share the property of projecting to the injection site, but further subdivisions may be established on the basis of dendrite morphometry, local axon branching, or other properties (51).

While more work and a larger sample size will be necessary to address this issue, several recent studies (52, 53) have identified distinct, previously covert intralaminar subcircuits. It seems plausible that continued work with an assortment of markers will yet reveal a high degree of pyramidal cell diversity (51).

5.2.3. Dendritic domains

Case 135 was the most favorable for assessing bouton distribution over the different dendritic domains of identified neurons in layers 2 or 3a. The results basically show contacts on all components (basal, apical, oblique, tuft). From cell 2, with the highest number of contacts, we had some impression that there were relatively fewer contacts on basal dendrites. From this and other neurons, we also had an impression of preferential targeting of the

middle sector of the basal dendrites. This may be significant in the context of how the synaptic distribution influences the firing properties of the postsynaptic neuron (54-56); but these observations will also require further confirmation.

5.3. Future directions

Several obvious future directions are immediately apparent. For example, a larger sample size is desirable, both of additional experimental material to confirm our current results, and of more extensive neuronal reconstructions, to better establish patterns of dendritic target preference. EM validation of contacts scored by CM, as already discussed, is necessary to establish a baseline confidence level.

Beyond that, mapping of identified cortical connections will need to be extended to other connectional systems, such as, intrinsic, amygdalo-cortical, and thalamo-cortical. This could be accomplished by using a similar experimental design, but with different injection sites. Alternatively to injections or in combination with these, there are global populational markers, such as VGluT1 (for cortical terminations) and VGluT2 (for thalamic terminations). Unfortunately, these have so far been more successful in rodent than in primate tissue. Thalamocortical connections in primate have previously been investigated by EM, by equating these with parvalbumin positive terminations. Possible confoundment with GABAergic local interneurons is avoided by using VGAT to selectively label inhibitory parvalbumin positive terminations, which are then subtracted out.

The role of long-distance connections in cortical microcircuitry, previously addressed by indirect methods (57), can be more directly assessed by newer technologies (58). We can safely predict that future investigations will be able to access connectional influences at the level of individual synapses and the rules for their target specificity and interactions (59, 60).

5.4. Implications

This line of work is directly relevant for investigations of the integrative and firing properties of individual neurons. We have emphasized target specificity; but better understanding of microcircuitry is also relevant to our ideas of columnar organization (how similar is the connectivity of different neurons within a columnar group?). It will directly advance the debate on area and neuronal diversity vs uniformity; and it may be critical to a finer classification of cortical connections. There have been classified according to laminar patterns (feedforward, feedback, lateral) or, especially in the corticothalamic system, as driving or modulatory. However, one can anticipate that additional data, especially concerning interactions at the synaptic level across dendritic microdomains, will significantly add to both the current taxonomy and concepts of connectivity.

6. ACKNOWLEDGEMENTS

7. REFERENCES

1. R. J. Douglas and K. A.C. Martin: Neuronal circuits of the neocortex. *Annu Rev Neurosci* 27, 419-451 (2004)

2. R.R. Johnson and A. Burkhalter: Microcircuitry of forward and feedback connections within rat visual cortex. *J Comp Neurol* 368, 383-398 (1996)

3. R.R. Johnson and A. Burkhalter: A polysynaptic feedback circuit in rat visual cortex. *J Neurosci* 17, 7129-7140 (1997)

4. T. Kaneko, R. Cho, Y. Li, S. Nomura and N. Mizuno: Predominant information transfer from layer III pyramidal neurons to corticospinal neurons. *J Comp Neurol* 423, 52-65 (2000)

5. M. Kuroda, J. Yokofujita and K. Murakami: An ultrastructural study of the neural circuit between the prefrontal cortex and the mediodorsal nucleus of the thalamus. *Prog Neurobiol* 54, 417-458 (1998)

6. A. Peters: Examining neocortical circuits: Some background and facts. *J Neurocytol* 31, 183-193 (2002)

7. E. L. White: Cortical circuits. Synaptic organization of the cerebral cortex; structure, function and theory, 1 edn. *Birkhauser*, Boston (1989)

8. E. L. White: Specificity of cortical synaptic connectivity: Emphasis on perspectives gained from quantitative electron microscopy. *J Neurocytol* 31, 195-202 (2002)

9. J.V. Le Be, G. Silberberg, Y. Wang and H. Markram: Morphological, electrophysiological, and synaptic properties of corticocallosal pyramidal cells in the neonatal rat neocortex. *Cereb Cortex* 17, 2204-2213 (2007)

10. A.P. Bannister and A.M. Thomson: Dynamic properties of excitatory synaptic connections involving layer 4 pyramidal cells in adult rat and cat neocortex. *Cereb Cortex* 17, 2190-2203 (2007)

11. J.L. Freese and D.G. Amaral: Synaptic organization of projections from the amygdala to visual cortical areas TE and V1 in the macaque monkey. *J Comp Neurol* 496, 655-667 (2006)

12. F.G. Wouterlood, T. Bockers and M.P. Witter: Synaptic contacts between identified neurons visualized in the confocal laser scanning microscope. Neuroanatomical tracing combined with immunofluorescence detection of post-synaptic density proteins and target neuron-markers. *J Neurosci Methods* 128, 129-142 (2003)

13. F.G. Wouterlood, T. Van Haeften, M. Eijkhoudt, L. Baks-Te-Bulte, P.H. Goede and M.P. Witter: Input from the presubiculum to dendrites of layer-V neurons of the medial entorhinal cortex of the rat. *Brain Res* 1013, 1-12 (2004)

14. F. G. Wouterlood, A. J. Boekel, G. A. Meijer and J. A. M. Belien: Computer-assisted estimation in the CNS of 3D multimarker "overlap" or "touch" at the level of individual

nerve endings: a confocal laser scanning microscope application. *J Neurosci Res* 85, 1215-1228 (2007)

15. R. Tomioka, and K. S. Rockland: Improved Golgi-like visualization in retrogradely projecting neurons after EGFP-adenovirus infection in adult rat and monkey. *J Histochem Cytochem* 54, 539-548 (2006)

16. R. Tomioka, and K. S. Rockland: Long-distance corticocortical GABAergic neurons in the adult monkey white and gray matter. *J Comp Neurol* 505, 526-538 (2007)

17. N. Ichinohe and K.S. Rockland: Zinc-enriched amygdalo- and hippocampo-cortical connections to the inferotemporal cortices in macaque monkey. *Neurosci Res* 53, 57-68 (2005)

18. P. Lavenex, W.A. Suzuki and D.G. Amaral: Perirhinal and parahippocampal cortices of the macaque monkey: Intrinsic projections and interconnections. *J Comp Neurol* 472, 371-394 (2004)

19. C.L. Martin-Elkins and J.A. Horel: Cortical afferents to behaviorally defined regions of the inferior temporal and parahippocampal gyri as demonstrated by WGA-HRP. *J Comp Neurol* 321, 177-192 (1992)

20. K.S. Saleem, K. Tanaka and K.S. Rockland: Specific and columnar projection from area TEO to TE in the macaque inferotemporal cortex. *Cereb Cortex* 3, 454-464 (1993)

21. K.S. Saleem and K. Tanaka: Divergent projections from the anterior inferotemporal area TE to the perirhinal and entorhinal cortices in the macaque monkey. *J Neurosci* 16, 4757-4775 (1996)

22. K.S. Saleem, J.L. Price and T. Hashikawa: Cytoarchitectonic and chemoarchitectonic subdivisions of the perirhinal and parahippocampal cortices in macaque monkeys. *J Comp Neurol* 500, 973-1006 (2007)

23. W. Suzuki, K.S. Saleem and K. Tanaka: Divergent backward projections from the anterior part of the inferotemporal cortex (area TE) in the macaque. *J Comp Neurol* 422, 206-228 (2000)

24. W.A. Suzuki and D.G. Amaral: Perirhinal and parahippocampal cortices of the macaque monkey: cortical afferents. *J Comp Neurol* 350, 497-533 (1994)

25. W.A. Suzuki and D.G. Amaral: Perirhinal and parahippocampal cortices of the macaque monkey: cytoarchitectonic and chemoarchitectonic organization. *J Comp Neurol* 463, 67-91 (2003)

26. M.J. Webster, L.G. Ungerleider and J. Bachevalier: Connections of inferior temporal areas TE and TEO with medial temporal-lobe structures in infant and adult monkeys. *J Neurosci* 11, 1095-1116 (1991)

27. M. Yoshida, Y. Naya and Y. Miyashita: Anatomical organization of forward fiber projections from area TE to perirhinal neurons representing visual long-term memory in monkeys. *Proc Natl Acad Sci U S A* 100, 4257-4262 (2003)

28. Y.M. Zhong and K.S. Rockland: Connections between the anterior inferotemporal cortex (area TE) and CA1 of the hippocampus in monkey. *Exp Brain Res* 155, 311-319 (2004)

29. D.J. Felleman and D.C. Van Essen: Distributed hierarchical processing in the primate cerebral cortex. *Cereb Cortex* 1, 1-47 (1991)

30. K.S. Rockland and D.N. Pandya: Laminar origins and terminations of cortical connections of the occipital lobe in the rhesus monkey. *Brain Res* 179, 3-20 (1979)

31. J.S. Lund: Organization of neurons in the visual cortex, area 17, of the monkey (Macaca mulatta). *J Comp Neurol* 147, 455-496 (1973)

32. K.S. Saleem and N.K. Logothetis: A combined MRI and histology atlas of the rhesus monkey brain in stereotaxic coordinates. Elsevier, Amsterdam (2007)

33. W.A. Suzuki and D.G. Amaral: Where are the perirhinal and parahippocampal cortices? A historical overview of the nomenclature and boundaries applied to the primate medial temporal lobe. *Neuroscience* 120, 893-906 (2003)

34. Y.M. Zhong and K.S. Rockland: Inferior parietal lobule projections to anterior inferotemporal cortex (area TE) in macaque monkey. *Cereb Cortex* 13, 527-540 (2003)

35. J. DeFelipe and I. Farinas: The pyramidal neuron of the cerebral cortex: morphological and chemical characteristics of the synaptic inputs. *Prog Neurobiol* 39, 563-607 (1992)

36. J.C. Anderson and K.A. Martin: Does bouton morphology optimize axon length? *Nat Neurosci* 4, 1166-1167 (2001)

37. H. Hioki, H. Kameda, H. Nakamura, T. Okunomiya, K. Ohira, K. Nakamura, M. Kuroda, T. Furuta and T. Kaneko: Efficient gene transduction of neurons by lentivirus with enhanced neuron-specific promoters. *Gene Ther* 14, 872-882 (2007)

38. D.D. Stettler, H. Yamahachi, W. Li, W. Denk and C.D.Gilbert. Axons and synaptic boutons are highly dynamic in adult visual cortex. *Neuron* 49, 877-887 (2006)

39. I.R. Wickersham, S. Finke, K.K. Conzelmann and E.M. Callaway: Retrograde neuronal tracing with a deletion-mutant rabies virus. *Nat Methods* 4, 47-49 (2007)

40. B. Amirikian: A phenomenological theory of spatially structured local synaptic connectivity. *PLoS Comput Biol* 1, 74-85 (2005)

41. T. Binzegger, R.J. Douglas and K.A. Martin: Axons in cat visual cortex are topologically self-similar. *Cereb Cortex* 15, 152-165 (2005)

42. V. De Paola, A. Holtmaat, G. Knott, S. Song, L. Wilbrecht, P. Caroni and K. Svoboda: Cell type-specific structural plasticity of axonal branches and boutons in the adult neocortex. *Neuron* 49, 861-875 (2006)

43. C. Portera-Cailliau, R.M. Weimer, V. De Paola, P. Caroni and K. Svoboda. Diverse modes of axon elaboration in the developing neocortex. *PLoS Biol* 3, 1-15 (2005)

44. A. Stepanyants, P.R. Hof and D.B. Chklovskii: Geometry and structural plasticity of synaptic connectivity. *Neuron* 34, 275-288 (2002)

45. A. Stepanyants, and D. B. Chklovskii: Neurogeometry and potential synaptic connectivity. *Trends Neurosci* 28, 387-394 (2005)

46. G. M. Shepherd, A. Stepanyants, I. Bureau, and D. B. Chklovskii, K. Svoboda: Geometric and functional organization of cortical circuits. *Nat Neurosci* 8, 782-790 (2005)

47. A.M. Thomson, A.P. Bannister, A. Mercer and O.T. Morris: Target and temporal pattern selection at neocortical synapses. *Philos Trans R Soc Lond B Biol Sci* 357, 1781-1791 (2002)

48. T.R. Sato, N.W. Gray, Z.F. Mainen and K. Svoboda: The Functional Microarchitecture of the Mouse Barrel Cortex. *PLoS Biol* 5, e189 (2007)

49. K.S. Rockland and N. Ichinohe: Some thoughts on cortical minicolumns. *Exp Brain Res* 158, 265-277 (2004)

50. J. DeFelipe, G.N. Elston, I. Fujita, J. Fuster, K.H. Harrison, P.R. Hof, Y. Kawaguchi, K.A. Martin, K.S. Rockland, A.M. Thomson, S.S. Wang, E.L. White and R. Yuste: Neocortical circuits: evolutionary aspects and specificity versus non-specificity of synaptic connections. Remarks, main conclusions and general comments and discussion. *J Neurocytol* 31, 387-416 (2002)

51. S.B. Nelson: Cortical microcircuits: diverse or canonica. *Neuron* 36, 19-27 (2002)

52. Y. Yoshimura, J.L. Dantzker and E.M. Callaway: Excitatory cortical neurons form fine-scale functional networks. *Nature* 433, 868-873 (2005)

53. I. Bureau, P.F. von Saint, K. Svoboda: Interdigitated paralemniscal and lemniscal pathways in the mouse barrel cortex. *PLoS Biol* 4, e382 (2006)

54. T. Euler and W. Denk: Dendritic processing. *Curr Opin Neurobiol* 11, 415-422 (2001)

55. A. Frick and D. Johnston: Plasticity of dendritic excitability. *J Neurobiol* 64, 100-115 (2005)

56. U. Gordon, A. Polsky and J. Schiller: Plasticity compartments in basal dendrites of neocortical pyramidal neurons. *J Neurosci* 26, 12717-12726 (2006)

57. T. Binzegger, R.J. Douglas, K.A. Martin: A quantitative map of the circuit of cat primary visual cortex. *J Neurosci* 24, 8441-8453 (2004)

58. L. Petreanu, D. Huber, A. Sobczyk and K. Svoboda: Channelrhodopsin-2-assisted circuit mapping of long-range callosal projections. *Nat Neurosci* 10, 663-668 (2007)

59. Y. Humeau, C. Herry, N. Kemp, H. Shaban, E. Fourcaudot, S. Bissiere and A. Luthi: Dendritic spine heterogeneity determines afferent-specific Hebbian plasticity in the amygdala. *Neuron* 45, 119-131 (2005)

60. K.A. Pelkey and C.J. McBain: Differential regulation at functionally divergent release sites along a common axon. *Curr Opin Neurobiol* 17, 366-373 (2007)

Abbreviations: AdSynEGFP: adenovirus vecor for enhanced green flurescent protein, with a synapsin I promoter, amts: anterior middle remporal sulcus, BDA: biotinylated dextran amine, EM: electron microscopy, TEa: anteior TE, TEav, TEad: anterior ventral (dorsal) TE, TEp: posterior TE, tmps: temporal middle posterior sulcus, VGluT1, VGluT2: vesicular glutamate transporter 1 (2)

Key Words: Cortical Microcircuit, Dendritic Spines, Dendritic Remodelling, Inferotemporal Cortex, Synapses, Viral Vector

Send correspondence to: Dr. Kathleen S. Rockland, Lab for Cortical Organization and Systematics, RIKEN Brain Science Institute, 2-1 Hirosawa, Wako-shi, Saitama, 351-0198 Japan, Tel.: 81-48-467-6427, Fax: 8148-467-6420, E-mail: rockland@brain.riken.jp